IIAT Instituto Internacional de Análise Térmica

Available online at www.bjta.iiatbr.org
Braz. J. Therm. Anal. Vol. 4 No. 4 (2015) 41 – 46
DOI: 10.18362/bjta.v4.i4.232

Brazilian Journal of Thermal Analysis BJTA

Thermal behavior of nicotinate of some bivalent transition metal ions in dry CO_2 and N_2 atmospheres

do Nascimento A. L. C. S[1*], Caires F. J., Colman T. A. D., Ionashiro M.

[1]*Instituto de Química, Universidade Estadual Paulista, CP 355, 14801-970 Araraquara, SP, Brazil*

Received data: 10/07/2015; **accepted data:** 11/11/2015
Available online: 31/12/2015

Abstract

Synthesis, characterization and thermal decomposition of bivalent transition metal nicotinates $M(C_6H_4NO_2)_2 \cdot nH_2O$ (M = Mn (II), Fe(II), Co(II), Ni(II), Cu(II) and Zn(II)), as well as the thermal decomposition of sodium nicotinate, were investigated employing simultaneous thermogravimetry and differential thermal analysis (TG-DTA), simultaneous thermogravimetry and differential scanning calorimetry (TG-DSC) coupled to infrared spectroscopy (FTIR) and complexometry. In both atmospheres, the thermal decomposition of sodium nicotinate up to 500 ºC, occurs with the formation of sodium carbonate and carbonaceous residue and up to 800 ºC the mass loss is still being observed. In CO_2 atmosphere the thermal decomposition of these compounds occurs in three consecutive steps, with the formation of the respective metal or metal oxides: MnO, FeO, CoO, Ni°, Cu° and ZnO. In N_2 atmosphere, the thermal decomposition also occurs, in three consecutive steps and only iron and cobalt compounds, with the formation of Fe_3O_4 and CoO, respectively, while the other compounds the mass loss is still being observed up to 1000 ºC.

Keywords: transition metals, nicotinate, thermal behaviour

1. Introduction

Nicotinic, 3-picoline or pyridine-3-carboxylic acid (Fig 1) is the biological precursor of the co-enzymes: nicotinamide adenine dinucleotide (NAD) and nicotinamide adenine dinucleotide phosphate (NADP).

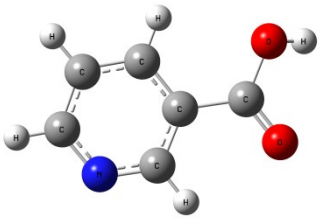

Figure 1. Structural formula of nicotinic acid.

The literature shows that the papers involving nicotinic acid and bivalent manganese, cobalt, nickel, copper and zinc reported the spectroscopic, thermogravimetric, magnetic studies and thermochemical behavior of solid nicotinic hydrazide [1,2], thermal decomposition of copper (II) nicotinate, isonicotinate and synthesis and characterization of copper (II) complexes with nicotinate in different coordination style [3,4], a new 2-D chiral coordination polymer of $[Zn(nicotinate)2]_n$ [5], simultaneous thermal analysis of a cobalt (II) complex with nicotinate [6], hydrothermal synthesis, crystal structures and properties of two 3-D network nickel nicotinate coordination polymers and hydrothermal synthesis, structural determination and thermal properties of 2-D cobalt-and nickel-based coordination polymers incorporating pendant-arm 3-pyridinecarboxylate ligands [7,8], synthesis, structures and properties of 3d/5d-4f metal complexes with novel polycationic chains [9], a pionner study on the anti-ulcer activies of copper nicotinate complex $[CuCl(HNA)_2]$ in experimental gastric ulcer induced by aspirin-pyloris ligation model (shay model) [10], Growth and characterization of a novel polymer of manganese (II) nicotinate single crystal [11] and thermal behavior of nicotinic acid, sodium nicotinate and its compounds with some bivalent transition metal ions [12].

In this paper, solid-state compounds of some bivalent transition metal ions (i.e. Mn, Fe, Co, Ni, Cu and Zn) with nicotinate were prepared. These compounds were investigated by means of complexometric, simultaneous thermogravimetry and differential thermal analysis (TG-DTA) in CO_2 and N_2 atmospheres and simultaneous thermogravimetry and differential scanning calorimetry (TG-DSC) coupled to infrared spectroscopy (FTIR), since the use of the coupled techniques makes possible a correct interpretation for the mechanism of a thermally induced reaction, involving the formation of gaseous species evolved during the thermal decomposition [13]. This work is primarily a continuation and extension of a previously reported study [12].

2. Experimental

The nicotinic acid ($C_6H_4NO_2$) with 99.5% purity was obtained from Sigma and it was used as received. Aqueous solution of sodium nicotinate 0.1 mol L^{-1} was prepared by neutralization of an aqueous solution of nicotinic acid with sodium hydroxide solution 0.1 mol L^{-1}. Aqueous solutions of bivalent metal ions 0.1 mol L^{-1} were prepared by dissolving

* **Corresponding author:** Tel.: +55-16-3301-9617
E-mail address: nascimento.a.l.c@gmail.com (A. L. C. S do Nascimento)

© 2015 Published by IIAT – Instituto Internacional de Análise Térmica

the corresponding chloride (Mn(II), Co(II), Ni(II)) or sulphate (Fe(II), Cu(II), Zn(II)).

The solid-state compounds were prepared by adding slowly with continuous stirring 100 mL sodium nicotinate solution 0.1 mol L^{-1} to 50 mL of the respective metal ions solutions 0.1 mol L^{-1} heated up to near ebullition, following the same procedure already described [12].In the solid-state metal ions, hydration water and nicotinate contents were determined from TG curves obtained in CO_2 atmosphere. The metal ions were also determined by complexometric with standard EDTA solution after igniting the compounds to the respective oxides and their dissolution in hydrochloric acid solution [14, 15].

Carbon, hydrogen and nitrogen contents were determined by calculations based on the mass losses of the TG curves obtained in CO_2 atmosphere, since the water and ligand lost in the thermal decomposition occurred with the formation of the respective metal or oxides with stoichiometry known, as final residue.

Simultaneous TG-DTA curves were recorded on a model SDT 2960 Thermal analysis system from TA Instruments. The purge gases were CO_2 and N_2 flow of 50 and 100 mL min-1, respectively. A heating rate of 10 ºC min-1 was adopted, with samples weighing about 7 mg. Alumina crucibles were used for recording the TG-DTA curves.

The measurements of the gaseous products were carried out by using a TG-DSC Mettler Toledo coupled to FTIR spectrophotometer Nicolet with gas cell and DTGS KBr detector.

The furnace and the heat gas cell (250 ºC) were coupled through a heated (200 ºC) 120 cm stainless steel line transfer with 3 mm diameter both purged with dry N_2 (50 mL min^{-1}). The FTIR spectra were recorded with 16 scans per spectrum at a resolution of 4 cm^{-1}.

3. Results and Discussion

The TG-DTA curves of sodium nicotinate in CO_2 and N_2 atmospheres are shown in Fig. 2 a, a*. In both atmospheres, the TG curve shows that the thermal decomposition occurs in two consecutive steps between 410 and 780 ºC, in spite of the mass loss is still being observed. The endothermic peak at 410 ºC (CO_2, N_2) without mass loss in the TG curve is attributed to the fusion of the compound, in agreement with the ref. [12].

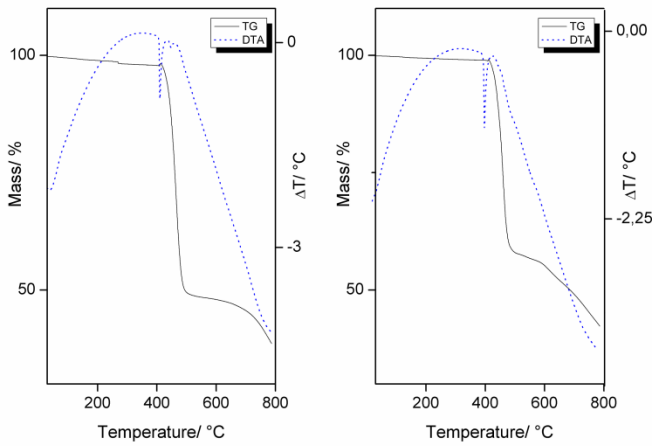

Figure 2. Simultaneous TG-DTA curves of sodium nicotinate in (a) CO_2 (m = 3.0527 mg) and (a*) N_2 atmospheres (m = 3.2556 mg).

These curves also show a great similarity in the TG-DTA profiles in both atmospheres, although the mass loss in each step of the TG curve is characteristic of each atmosphere.

For CO_2 atmosphere, the first step between 410 and 500 ºC, with loss of 51.84%, corresponding to a small endothermic peak at 447 ºC is attributed to the thermal decomposition with the formation of a mixture of sodium carbonate and carbonaceous residue. The second step between 600 and 780 ºC, with loss of 9.56% without thermal event is attributed to the partial pyrolysis of the carbonaceous residue.

For N_2 atmosphere, the mass losses occur between 410-500 ºC and 500-780 ºC, without thermal event with losses of 41.96% and 17.71%, respectively. The first mass loss is also attributed to the thermal decomposition with the formation of a mixture of sodium carbonate and carbonaceous residue and the second one to the partial pyrolysis of the carbonaceous residue.

For the synthesized compounds the analytical and thermoanalytical (TG) data are shown in Table 1.

Table 1. Analytical and thermoanalytical (TG) data for the $M(C_6H_4NO_2)_2{\cdot}nH_2O$ compounds in CO_2 atmosphere.

Compound	Metal oxide/ %			L (Lost)/ %		Water/ %		C/ %		N/ %		H/ %		Final Residue
	Calc.	EDTA	TG	Calc.	TG	Calc.	TG	Calc.	TG	Calc.	TG	Calc.	TG	
$Mn(L)_2{\cdot}2H_2O$	21.16	21.25	21.40	68.09	67.58	10.75	11.02	43.00	42.87	8.36	8.33	3.36	3.61	MnO
$Fe(L)_2{\cdot}3.5H_2O$	19.79	20.02	20.50	62.84	62.26	17.37	17.24	39.69	39.34	7.72	7.65	4.17	4.13	FeO
$Co(L)_2{\cdot}4H_2O$	19.97	20.01	19.54	60.82	61.07	19.21	19.39	38.41	38.62	7.47	7.51	4.31	4.33	CoO
$Ni(L)_2{\cdot}4.5H_2O$	15.29	15.40	15.31	63.59	63.93	21.12	20.76	37.53	37.52	7.30	7.30	4.47	4.47	Ni
$Cu(L)_2{\cdot}0.4H_2O$	20.18	20.50	20.33	77.53	77.50	2.29	2.17	45.76	45.67	8.90	8.88	2.82	2.81	Cu
$Zn(L)_2{\cdot}0.23H_2O$	25.94	26.10	25.91	72.74	72.79	1.32	1.30	45.94	45.96	8.93	8.93	2.37	2.37	ZnO

These results permitted to stablish the stoichiometry of these compounds, which are in agreement with the general formula $M(L)_2$. nH_2O, where M represents bivalent manganese, iron, cobalt, nickel, copper, zinc, L is nicotinate and n = 4.5 (Ni), 4 (Co), 3.5 (Fe), 2 (Mn), 0.4 (Cu) and 0.23 (Zn).

The simultaneous TG-DTA curves of the synthesized compounds in CO_2 and N_2 atmospheres are shown in Fig. 2 in CO_2 (a-f) and N_2 (a* - f*), respectively. In both atmospheres, these curves show mass losses in steps characteristic of each compound and thermal events corresponding to these losses or due physical phenomenon. These curves also show a great similarity in the TG-DTA profiles as much in CO_2 as in N_2 atmosphere up to 475 ºC (Mn, Zn), 450 ºC (Fe, Co, Ni) and 300 ºC (Cu). This similarity suggests that the thermal decomposition mechanism for each compound must be the same.

Thus, in both atmospheres the thermal stability of the hydrated compounds (I), as well as of the anhydrous ones, as shown by TG-DTA curves depends on the nature of the metal ions, and they follow in both atmospheres the order:

$$Mn > Co \cong Ni > Fe > Cu \text{ (I)}$$

$$Mn > Co > Zn > Ni > Fe > Cu \text{ (II)}$$

The TG-DTA curves also show that the thermal behavior of the compounds is heavily dependent on the nature of the metal ion and so the features of each of these compounds are discussed individually.

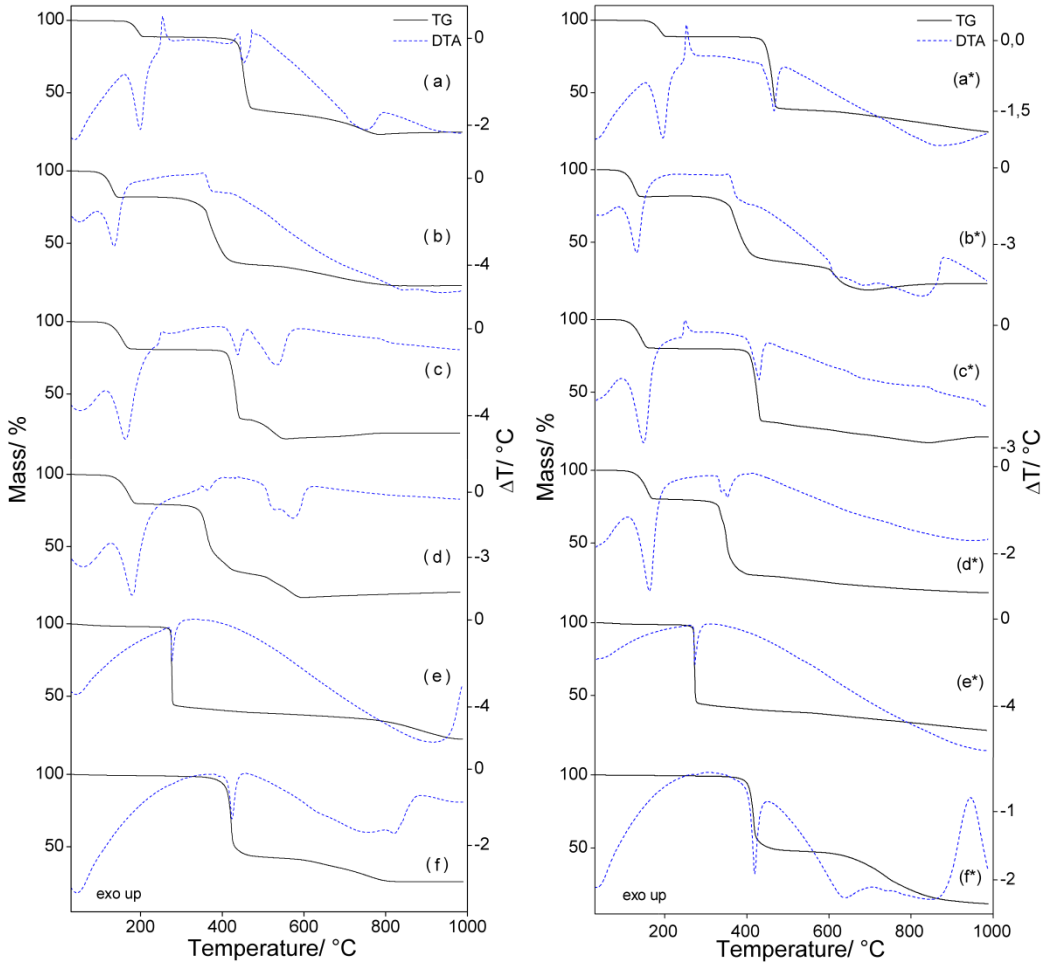

Figure 3. Simultaneous TG-DTA curves of the synthesized compounds in (a-f) CO_2 (sample masses: Mn = 7.0602 mg, Fe = 7.0283 mg, Co = 7.0929 mg, Ni = 7.0076 mg, Cu = 6.9630 mg and Zn = 7.0297 mg) and (a-f*) N_2 atmospheres (sample masses: Mn = 7.0044 mg, Fe = 7.0526 mg, Co = 7.0397 mg, Ni = 7.0193 mg, Cu = 7.0792 mg and Zn = 7.0102 mg).

3.1. Manganese compound

The simultaneous TG-DTA curves in CO_2 and N_2 atmospheres are shown in Fig. 3 a, a*. In both atmospheres these curves show mass losses in three steps, between 150 – 780 ºC (CO_2) and 150 - > 1000 ºC (N_2) and thermal events corresponding to these losses or due to physical phenomenon. The first mass loss between 150 and 210 ºC in both atmospheres is attributed to dehydration with loss of 2 H2O (Calcd. = 10.75%, TG = 11.02% (CO_2), 11.01% (N_2). The anhydrous compound is stable up to 390 ºC, and above this temperature the thermal decomposition occurs in two consecutive steps.

For CO_2 atmosphere, calculations based on the mass loss up to 780 ºC, are in agreement with the formation of MnO, as residue (Calcd. = 78.84%, TG = 78.80%). The small mass gain between 780 and 1000 ºC is attributed to the oxidation of MnO, with the formation of Mn3O4, as residue (Calcd. = 1.59%, TG = 1.52%).

For N_2 atmosphere, the mas loss is still being observed up to 1000 ºC. The sharp exothermic peak at

255 ºC (CO_2) or 253 ºC (N_2), without mass loss in the TG curve is attributed to irreversible transition phase, as already observed in the thermal decomposition of this compound in air atmosphere [12].

3.2. Iron compound

The simultaneous TG-DTA curves in CO_2 and N_2 atmosphere are shown in Fig. 3 b, b*. These curves show mass losses in three consecutive steps between 70 – 850 ºC (CO_2) and 75 – 690 ºC (N_2). The first mass loss between 70 – 154 ºC (CO_2) and 75 – 140 ºC (N2), corresponding to an endothermic peak at 134 ºC (CO_2) and 131 ºC (N_2) is attributed to the dehydration with loss of 3.5 H2O (Calcd. = 17.37%, TG = 17.24% (CO_2), 17.23% (N_2)). In both atmospheres the anhydrous compound is stable up to 285 ºC and above this temperature the thermal decomposition occurs in two consecutive steps up to 840 ºC (CO_2) and 690 ºC (N_2).

For CO_2 atmosphere, calculations based on the mass loss 840 ºC suggest the formation of FeO, as residue (Calcd. = 80.21%, TG = 79.70%) and based on the residue color (black) and magnetic property.

For N2 atmosphere, calculations based on the mass loss up to 690 ºC, also suggests the formation of a mixture of Fe° and FeO in no simple stoichiometric relation (Calcd. = Fe° = 84.62%, FeO = 80.21%, TG = 82.52%). The mass gain (4.14%), between 690 at 1000 ºC is FeO to Fe3O4. The formation of FeO and Fe3O4 was also based on the residue color (black) and magnetic property.

3.3. Cobalt compound

The simultaneous TG-DTA curves in CO_2 and N_2 atmospheres are shown in Fig. 3 c, c*. These curves show mass losses in three consecutive steps between 95 – 550 ºC (CO_2) and 90 -840 ºC (N_2). The first mass loss between 90 – 175 ºC (CO_2) and 90 – 165 ºC (N_2), corresponding to and endothermic peak at 165 ºC (CO_2) and 148 ºC (N_2) is attributed to dehydration with loss of 4 H2O (calcd. = 19.21%, TG = 19.39 (CO_2), 18.98% (N_2). The anhydrous compound is stable up to 380 ºC (CO_2) and 375 ºC (N_2), and above this temperature the thermal decomposition occurs in two consecutive steps up to 550 ºC (CO_2) and 840 ºC (N_2).

For CO_2 atmosphere, the mass loss up to 550 ºC, suggests the formation of CoO, as residue (Calcd. = 80.03%; TG = 80.26%). The mass gain between 550 and 800 ºC is attributed to the oxidation reaction of CoO to Co3O4 (Calcd. = 1.42%, TG = 1.58).

For N_2 atmosphere, the mass loss up to 840 ºC, is in agreement with the formation of Co° as residue (Calcd. = 84.43%, TG = 84.73%). The mass gain between 840 and 980 ºC is attributed to the oxidation of Co to CoO (Calcd. = 4.22%, TG = 4.19%). The exothermic peak at 255 ºC (CO_2) or 249 ºC (N_2), without mass loss in the TG curve is attributed to the irreversible transition phase, in agreement with the result of ref. [12].

3.4. Nickel compound

The simultaneous TG-DTA curves in CO_2 and N_2 atmospheres are shown in Fig. 3 d, d*. These curves also show mass losses in three consecutive steps between 90 – 600 ºC (CO_2) and 90 - > 1000 ºC (N_2). The first mass loss between 90 – 195 ºC (CO_2) and 90 – 75 ºC (N_2), corresponding to an endothermic peak at 178 ºC (CO_2) and 163 ºC (N_2) is attributed to dehydration with loss of 4.5 H_2O (Calcd. = 21.12%, TG = 20.76% (CO_2), 21.03% (N2). The anhydrous compound is stable up to 290 ºC in both atmospheres and above this temperature up to 600 ºC (CO_2) and > 1000 ºC (N_2) the thermal decomposition occurs in two consecutive steps.

For CO_2 atmosphere the mass loss up to 600 ºC is in agreement with the formation of Ni°, as residue (Calcd. = 84.71%, TG = 84.69%). The mass gain (3.15%) between 600 and 980 is attributed to partial oxidation of Ni° to NiO, with formation of a mixture of Ni°.NiO in no simple stoichiometric relation (Calcd. = 84.71% (Ni), 80.55% (NiO), TG = 81.54%). For N2 atmosphere, the mass loss is still observed up to 1000 ºC.

3.5. Copper compound

The simultaneous TG-DTA curves in CO_2 and N_2 atmospheres are shown in Fig. 3 e, e*. These curves show mass losses in three consecutive steps between 40 – 980 ºC (CO_2) and 60 - > 1000 ºC (N_2). The small mass loss observed between 40 – 200 ºC (CO_2) and 60 – 150 ºC (N_2), without thermal event is attributed to the loss of adsorbed water, which correspond to 0.4 H2O (CO_2) (Calcd. = 2.29%, TG = 2.17%) and 0.25 H2O (N_2) (Calcd. = 1.44%, TG = 1.59%).

The anhydrous compound is stable up to 240 ºC in both atmospheres and above this temperature up to 980 ºC (CO_2) and > 1000 ºC (N_2), the mass loss occurs in two consecutive step, being the first step a fast process followed by slow one. For CO_2 atmosphere the mass loss up to 980 ºC is in agreement with the formation of Cu° as final residue (Calcd. = 79.82%, TG = 79.67%), while for N_2 atmosphere the mass loss is still being observed up to 1000 ºC.

3.6. Zinc compound

The simultaneous TG-DTA curves in CO_2 and N2 atmospheres are shown in Fig. 3 f, f*. These curves show mass losses in three (CO_2) or two (N_2) steps between 70 – 840 ºC and 330 - > 1000 ºC, respectively. For CO2 atmosphere, the first mass loss that occurs slow between 70 and 250 ºC, without thermal event is attributed to the loss of adsorbed water, which correspond to 0.23 H20 (Calcd. = 1.32%, TG = 1.31%). In both atmospheres, the anhydrous compound is stable up to 340 ºC, and above this temperature the mass losses occur in two consecutive steps up to 840 ºC (CO_2) and 980 ºC (N_2).

For CO_2 atmosphere the mass loss up to 840 ºC is in agreement with the formation of ZnO, as final residue (Calcd. = 74.07%, TG = 74.09%). For N2 atmosphere, the total mass loss of 88.14% suggests that during the thermal decomposition must occur the formation a mixture of Zn° and ZnO in no simple stoichiometric relation and evaporation of Zn° up to 980 ºC (mp = 420 ºC, bp = 907 ºC).

The X-ray diffraction powder patterns of the final residue, was not obtained due to the small mass of the final product of thermal decomposition. For the compounds where the mass gain was observed in the last step of the TG curve, the oxidation reaction occurs, probably because the equipment is not hermetically sealed and/or presence of oxygen in the N_2 and CO_2 which were used as purge gas.

In the thermal decomposition of these compounds, where the TG curve shows mass loss and no thermal event corresponding to this loss is observed in the DTA curve, undoubtedly is because the mass loss occurs slowly and the heat involved is not sufficient to produce a thermal event.

The temperature ranges, mass losses and the peak temperatures observed in each step of the TG-DTA curves in CO_2 and N_2 atmospheres are shown in Table 2.

Table 2. Temperatures Ranges Θ, mass losses (m) and peak temperatures (P) observed for each steps of TG-DTA curves of the $M(L)_2{\cdot}nH_2O$ compounds where M = bivalent transition metal ions, L = nicotinate

Compound		Steps							
		First step		Second step		Third step		Mass gain	
		CO_2	N_2	CO_2	N_2	CO_2	N_2	CO_2	N_2
$Mn(L)_2{\cdot}2H_2O$	Θ/°C	150-210	150-210	390-475	390-490	475-780	490-1000	780-1000	___
	m/(%)	11.02	11.01	49.87	50.13	17.91	15.69	1.32	___
	P/(°C)	200	194	452	466	750	875	___	___
$Fe(L)_2{\cdot}3.5H_2O$	Θ/°C	70-150	75-140	285-450	285-425	450-840	425-690	840-1000	690-1000
	m/(%)	17.24	17.23	47.30	42.40	15.16	22.89	0.34	4.14
	P/(°C)	134	131	380, 405	400	___	625	880(exo)	___
$Co(L)_2{\cdot}4H_2O$	Θ/°C	95-175	90-165	385-450	375-450	450-550	450-840	500-800	840-980
	m/(%)	19.39	18.98	47.98	51.02	12.89	14.73	3.84	4.19
	P/(°C)	165	148	437	431	535	___	___	___
$Ni(L)_2{\cdot}4H_2O$	Θ/°C	90-195	90-175	290-470	290-400	470-600	400-1000	600-1000	___
	m/(%)	20.76	21.03	47.62	50.65	16.31	12.51	3.15	___
	P/(°C)	178	163	363	352	572	___	___	___
$Cu(L)_2{\cdot}0.4H_2O$	Θ/°C	40-200	60-150	240-290	240-290	290-985	290-1000	___	___
	m/(%)	2.17	1.59	54.41	54.16	23.09	18.20	___	___
	P/(°C)	___	___	276	273	___	___	___	___
$Zn(L)_2{\cdot}H_2O$	Θ/°C	50-280	340-470	340-485	470-980	485-840	___	___	___
	m/(%)	1.31	50.61	51.83	37.53	17.95	___	___	___
	P/(°C)	___	418	425	632	755, 821	___	___	___

The gaseous products evolved during the thermal decomposition of the compounds studied in this work, in N2 atmosphere were monitored by FTIR, and in all the compounds water, carbon monoxide, carbon dioxide and pyridine were detected. The IR spectra of the gaseous products evolved during the thermal decomposition of cobalt compound, as representative of all the compounds are shown Fig. 4.

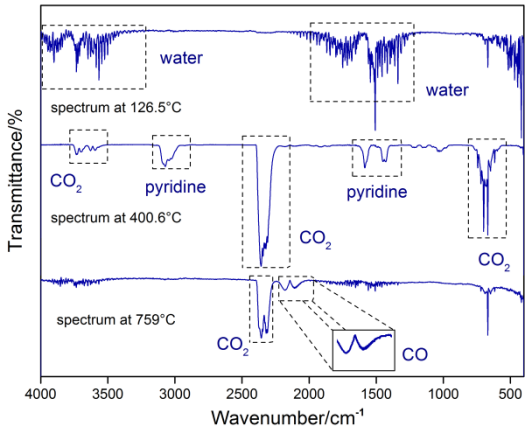

Figure 4. IR spectra of the gaseous products evolved during the thermal decomposition of cobalt compound: $Co(L)_2{\cdot}4H_2O$, as representative all the nicotinates compounds studied in this work.

4. Conclusion

The thermal decomposition of sodium nicotinate in CO_2 and N_2 atmospheres, up to 780 ºC occurs with the formation of mixture of sodium carbonate and carbonaceous residue, although the mass loss is still being observed up to this temperature.

From TG curve in CO2 atmosphere and complexometry results, as well as the carbon, hydrogen and nitrogen contents determined from TG curve, a general formula could be established for the synthesized compounds.

The TG-DTA curves also provided previously unreported information about the thermal stability and the thermal decomposition of these compounds in CO_2 and N_2 atmospheres.

The monitoring of the evolved gases during the thermal decomposition of the compounds studied in this work occurs with release of H_2O, CO, CO_2 and pyridine.

Acknowledgments

The authors thank FAPESP, CNPq and CAPES Foundations (Brazil) for financial support.

References

[1] Kleinstein A., Webb G. A. Spectroscopic, thermogravimetric and magnetic studies on some metal complexes with pyridine carboxylic acids. J Inorg Nucl Chem. 1971:33:405-12.

[2] Sekkina M. M. A., El-Azm M. G. A. Thermochemical behaviour of solid nicotinic hydrazide metal complexes in correlation with their stoichiometry. Thermochim Acta. 1984:77:211-18.

[3] Sileo E.E., Morando P. J., Vedova C. O. D., Blesa M. A. The thermal decomposition of copper (II) nicotinate and isonicotinate. Thermochim Acta. 1989:138: 233-39.

[4] Nie F., Deng Y., Li Y., Zhao Y. Synthesis and characterization of copper (II) complexes with nicotinate in different coordenation style. J Inorg Biochem. 2003:96:201.

[5] Lu J. Y., Kohler E. E. A new 2-D chiral coordination polymer of {Zn(nicotinate)$_2$]n Inorg Chem Commun. 2002:5:600-01.

[6] Liu Y., Yu J., Zhao J., Zhaug H., Deng Y., Wang Z. Simultaneous thermal analysis of a cobalt (II) complex with nicotinate. Thermochim Acta. 2004:419:115-17.

[7] Wasson A. E., LaDuca R. L. Hydrothermal synthesis crystal structures of two 3-D network nickel nicotinate coordination polymers. Polyhedron. 2007:26:1001-11.

[8] Martin D. P., Springsteen C. H., LaDuca R. L. Hydrothermal synthesis, structural determination and thermal properties of 2-D-cobalt-based coordination polymers incorporating pendant-arm 3-pyridine carboxylate ligands. Inorg Chim Acta. 2007:360:599-606.

[9] Chen W. T., Ying S. M., Liu D. S., Luo Q. Y., Xu Y. P. Syntheses, structures and properties of 3d/5d-4f metal complexes with novel polycationic chains. Inorg Chem Acta. 2009:362:2379-85.

[10] Tourkey M. J. F. A., Abdul-Aziz K. K. A pioneer study on the anti-ulcer activities of copper nicotinate complex [CuCl(HNA)$_2$] in experimental gastric ulcer induced by aspirin-pyloris ligation model (Shay model). Biomed Pharmacother. 2009:63:194-201.

[11] Prasanna S., Bijini B. R., RajeudraBabu K., Eapen S. M., Deepa M., Nair C. M. K. Growth and characterization of a novel polymer of manganese (II) nicotinate single crystal, J. Cryst. Grow. 2011:333:36-9.

[12] Nascimento A. L. C. S., Caires F. J., Gomes D. J. C., Gigante A. C., Ionashiro M. Thermal behavior of nicotinic acid, sodium nicotinate and its compounds with some bivalent transition metal íons. Thermochim Acta. 2014:575:212-18.

[13] Materazzi S., Vecchio S. Recent Applications of Evolved Gas Analysis by Infrared Spectroscopy (IR-EGA). Appl Spectroscopy Rev. 2013:48:654-89.

[14] Flaschka H. A. EDTA Titrations. Pergamon Press, Oxford 1964.

[15] Oliveira C. N., Ionashiro M., Graner C. A. F. Titulação complexomentrica de zinco, cobre e cobalto. Ecl Quim. 1985:10:7-10.